Quantitative SPECT and planar ^{32}P bremsstrahlung imaging for dosimetry purpose –An experimental phantom study

M.R. Teimoori Sichani[1], M. Amoui[2], Sh. Akhlaghpoor[3*], M. Hosntalab[1]

[1]Department of Medical Radiation Engineering, Science and Research branch, Islamic Azad University, Tehran, Iran
[2]Department of Nuclear Medicine, Shahid Beheshti University of Medical Science, Tehran, Iran
[3]Noor Medical Imaging Center, Tehran, Iran

► ***Original article***

Corresponding author:
Dr. Shahram Akhlagpoor,
Fax: *+98 21 66466383*
E-mail:
akhlaghpoor@pardisnoor.com

Received: Nov. 2013
Accepted: Feb. 2014

Int. J. Radiat. Res., April 2014; 12(2): 129-138

ABSTRACT

Background: In this study, Quantitative ^{32}P bremsstrahlung planar and SPECT imaging and consequent dose assessment were carried out as a comprehensive phantom study to define an appropriate method for accurate Dosimetry in clinical practice. ***Materials and Methods***: CT, planar and SPECT bremsstrahlung images of Jaszczak phantom containing a known activity of ^{32}P were acquired. In addition, Phantom contour was determined for attenuation correction and image registration. Reconstructed SPECT slices were corrected for attenuation effect using two different methods: conventional Chang`s method and an expectation maximization algorithm followed by CT and SPECT image registration. Cumulated activity was calculated by a predefined calibration factor. Both attenuation correction algorithms were quantitatively assessed by the Monte Carlo SIMIND program. Acquired planar Bremsstrahlung images were quantified by the Conjugate View Method, as well. ***Results***: Calculated activities were statistically different among various quantification methods (P= 0.0001). When iterative expectation maximization algorithm and applied methods were used, mean calculated activity had the least difference with real activity of ±3%. ***Conclusion***: Quantitative ^{32}P Bremsstrahlung SPECT imaging could accurately determine administered activity and assess radiation dose if precise attenuation correction and appropriate registration with CT were done even without sophisticated scatter correction or when SPECT/CT machines are not available. Therefore, it has the potential of specific tumor/organ dosimetry in clinical practice. The best method for calculating activity is quantitative SPECT using iterative expectation maximization algorithm. Additionally, applied method for determining phantom contour was practical for attenuation correction and image registration.

Keywords: *Bremsstrahlung imaging, quantitative SPECT imaging, attenuation correction, Phosphorus-32, activity determination, dosimetry.*

INTRODUCTION

Radioembolization (RE) with pure beta emitters has recently become an attractive treatment for patients with either primary or metastatic hepatic cancer [(1)]. Since 2009, it has been started in Iran and more than 100 patients have been treated with particles of ^{32}P in our clinic. Advantages of ^{32}P particles are its availability and low cost in our country as well as promising results for RE [(2)]. Briefly, beta emitter particles are administrated through femoral artery via catheter and selectively reach to the tumor region. Hence, two

treatment bases are applied: embolization or occlusion of vessels feeding the tumor as well as internal radiation therapy. As injected radiopharmaceuticals are usually purely beta emitters, post-radioembolization Bremsstrahlung imaging could be done for delivery control [3-5]. In addition, delivered dose to tumor could be assessed by both planar and SPECT Bremsstrahlung images [6-10], though various parameters should be considered including attenuation, scatter, collimator-detector response as well as statistical noise due to low count density [6, 7]. Many studies reported that the most effective factor in SPECT quantification is attenuation [9-11]. Consequently, exact compensation for attenuation effect is the main stage for accurate quantification. Two different attenuation correction (AC) algorithms, conventional post-processing Chang's method and an intrinsic iterative processing method, could be performed for SPECT quantification [12, 13] which were compared in the current study.

On the other hand, it is necessary to precisely register attenuation maps and reconstructed SPECT images for accurate AC. Manual registration of CT and reconstructed SPECT slices is based on specified common landmarks. Since there is no appropriate anatomical landmark in Bremsstrahlung images, a former method [14] was applied in this study to determine phantom contour. Finally, proposed algorithms were experimentally assessed by phantom studies and proposed AC technique in SPECT study was quantitatively evaluated using Monte Carlo SIMIND program. All processing steps and calculations are done using Matlab home-made software. Planar images were also quantified using Conjugate View Method (CVM) [15] without any specific compensation for scatter photons and other parameters. Briefly, the objective of this study was to identify a comprehensive method for quantitative ^{32}P Bremsstrahlung imaging and subsequent tumor/ organ's dosimetry in clinical practice.

MATERIALS AND METHODS

Data acquisition

A Jaszczak phantom (or "elliptical phantom") consisting of a ^{32}P vial with the activity of 49.17 MBq in the center, filled with non-radioactive water(as scattering medium), was used for phantom study. CT images (Sensation 64, Siemens Medical Solution, Germany) of the phantom were acquired at 120 kVp and 35 mA. SPECT imaging was performed using a single-head gamma-camera (E-Cam, Siemens Medical Solutions, Germany) equipped with medium-energy collimator. Energy window setting was 100 keV ± 25% which demonstrates optimal resolution characteristic for ^{32}P [16]. SPECT images were acquired with 64 projections over 360° rotation of camera for the duration of 30 s/frame in 64×64 matrix size. Additionally, phantom's contour was determined (described below) to improve subsequent image registration.

Phantom contour determination

According to the former study [14], two external ^{99m}Tc sources, either containing 37 MBq in 2 cc syringe filled up to 0.5 cc, were placed directly on the collimator surface, just outside the field of view, on its right and left end. Using this arrangement, along with preset energy window of 100 keV ± 25%, Bremsstrahlung photons in the range of 87 keV to 112 keV would be imaged as well as 90° to 180° Compton scattered photons emitted from ^{99m}Tc sources (representing the energy of 110 keV and 90 keV, respectively). The latter part could outline the phantom or body contour.

Also two small ^{99m}Tc sources with activity of 2 MBq were placed on top of the phantom as landmarks for SPECT and CT image registration.

Two series of SPECT and planar images, with and without external ^{99m}Tc sources (^{99m}Tc sources on collimators), were acquired to evaluate count contribution due to the external sources.

SPECT reconstruction and image registration

SPECT images were reconstructed using Maximum Likelihood Expectation Maximization (MLEM) algorithm with only 5 iterations, as higher number of iterations resulted in more noisy images due to low count density.

Reconstructed transverse SPECT and CT slices were assumed as reference and target images, respectively, with a subsequent

transformation function for image registration. First, similar pairs of reconstructed SPECT and CT images were chosen with contribution of landmarks along Z axis and phantom contour. Resolution folding of CT images was done by applying a Gaussian filter on CT images. Registration of the selected pairs was done on a point-to-point basis using a rigid transformation function. Phantom contour and landmarks over phantom were also used to find similar points in both SPECT and CT images.

Other similar SPECT and CT slices were automatically selected using known slice thicknesses of both SPECT and CT images. CT series with the slice thickness of 1 mm was chosen to avoid creating intermediate CT slices [17]. Finally, calculated transformation function was applied to all appropriately matched CT and SPECT slices.

To assess accuracy of suggested registration algorithm, two evaluation coefficients, "Target Overlap" (TO) and "Dice Coefficient" (DC) [18-20] were measured.

$$TO = \frac{S \cap T}{T} \quad (1)$$

$$DC = 2\frac{S \cap T}{S + T} \quad (2)$$

Where S is the surface of the reference image and T is surface of target image. S and T are defined in figure 1.

As registration of phantom images was done by user pair points selection, it was done for 20 times and TO and DC were calculated each time.

Attenuation correction

Attenuation correction is the basis of quantitative SPECT, activity measurement and consequent dosimetry. Accordingly, compensation for attenuation effect was done on SPECT images using two different methods: Conventional Chang`s method [13] as a post-processing method and an iterative method [12] as an intrinsic processing method.

In Chang's method, SPECT images were initially reconstructed using filtered back projection (FBP) method ('Hanning' filter, Cutoff = 0.8) and correction factor for each pixel

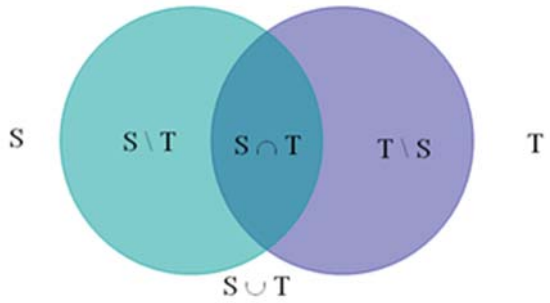

Figure 1. Schematic diagram of the definition for source and target overlap

was calculated using Chang`s applicable equation:

$$CF = \frac{1}{\frac{1}{N}\sum_{i=1}^{N} \mu_i} \quad (3)$$

Where CF is the correction factor for each pixel, $\int_i$ is the transmission at angle i from the voxel through the phantom to the surface of it and N is the total number of projections.

To compensate for attenuation effect with the iterative intrinsic method, MLEM reconstruction was applied (using pairs of attenuated projections/backprojections) [12] and 20 iterations were used to reach optimum quantitative accuracy. Attenuated projection for each angle was calculated using appropriate attenuation map (described below) and the projection was compared with real projection obtained from gamma camera in each iteration to update the reconstructed image.

MC simulation with SIMIND code

Intrinsic attenuation correction technique (AC during EM process) was evaluated by SIMIND MC code [21]. A digital phantom containing five hot spheres and background activity with the ratio "hot to background" of 5:1 was defined for quantitative and qualitative evaluation of the used AC method.

Attenuation maps

As two different AC methods were performed in this study, two different attenuation maps were applied. The first one was non-uniform attenuation map calculated by bilinear curve of Hounsfield Unit (HU) and Linear Attenuation Coefficient (LAC) [22]. HUs

were obtained using CT images of air (empty field), Jaszczak phantom filled with water and bone-equivalent phantom. LACs for photons with the energy of 100 keV were calculated using XCOM photon cross section database [23]. The HU to LAC curve was divided into two linear parts, first part was HUs less than HU of water and the second part was HUs more than HU of water. CT images of air and Jaszczak phantom filled with water were used to calculate the first part of curve (HU<0) and CT images of bone-equivalent phantom with different densities for second part (HU>0).

Second kind of attenuation map was uniform attenuation map which was created from non-uniform attenuation map. The first step was edge detection using "Canny" edge detection method [24]. Then, the mean attenuation coefficient within phantom area was calculated for each map. Next, uniform attenuation maps were created by applying mean attenuation coefficients within phantom contour for each map.

Planar quantification

180° opposed planar images, known as the conjugate view approach, transmission data through the subject and a system calibration factor were applied for in vivo quantitation. The conjugate view image pairs were typically anterior and posterior (A/P) images of the source region. CT images determined the real organ and body thicknesses. Effective linear attenuation coefficient for ^{32}P Bremsstrahlung photons was calculated by a separate phantom study: The Jaszczak phantom was filled up to different depths and located between the head of gamma camera and the syringe containing 74 MBq^{32}P and water. In addition, the syringe was placed directly front the gamma camera and imaged. Total counts in ROI on syringe area were determined for each image and effective linear attenuation coefficient was calculated by formula:

$$I = I_0 e^{-\mu x} \qquad (4)$$

Where I is the total counts in ROI with the water filled up to the depth of x and I_0 demonstrates primary counts in ROI before inserting Jaszczak phantom.

Two planar 180° opposed images, anterior and posterior, were acquired and a ROI was defined on either anterior or posterior image. The ROI was flipped horizontally to determine the region on the other image, as anterior and posterior images are exactly symmetric. Thicknesses of the phantom and source were determined using CT images and source activity was estimated using the following formula:

$$A = (R_A R_P)^{\frac{1}{2}} / \left[\frac{\sinh(\mu l/2)}{\mu l/2}\exp(-\frac{\mu L}{2})\right] E \qquad (5)$$

Where A is source activity in MBq, R_A and R_P are count rate in the ROI in anterior and posterior images, $\int$ is the effective linear attenuation coefficient in cm^{-1}, l and L are organ and body thickness in centimeter (which in this study are phantom and source thicknesses, respectively) and E is the calculated system calibration factor.

Activity measurement and dosimetry

First, a system calibration factor was calculated by imaging of a petri dish containing 49.17 MBq ^{32}P and water. This parameter actually indicated system sensitivity for imaging of ^{32}P Bremsstrahlung photons under described condition. Then, Volume of interest (VOI) was defined using CT or SPECT images in a user-based process in our written program. It was defined and counted on^{32}P source (inserted vial) for 20 times. Next, activity was estimated using total counts within each VOI and system calibration factor and compared with true ^{32}P activity.

Finally, delivered dose to the phantom was measured by mass calculation, using known voxel dimension, as well as calculated activity, assuming that all beta particles energy is absorbed at the phantom.

Activity measurement and dosimetry

First, a system calibration factor was calculated by imaging of a petri dish containing 49.17 MBq ^{32}P and water. This parameter actually indicated system sensitivity for imaging of ^{32}P Bremsstrahlung photons under described condition. Then, Volume of interest (VOI) was defined using CT or SPECT images in a

user-based process in our written program. It was defined and counted on ^{32}P source (inserted vial) for 20 times. Next, activity was estimated using total counts within each VOI and system calibration factor and compared with true ^{32}P activity.

Finally, delivered dose to the phantom was measured by mass calculation, using known voxel dimension, as well as calculated activity, assuming that all beta particles energy is absorbed at the phantom.

Software and statistical analysis

Matlab home-made software was used for SPECT reconstruction, AC, creating attenuation maps and image registration as well as all subsequent calculations concerning activity and dose measurements.

For statistical analysis, nonparametric method of Friedman for multiple repeated measurements was performed to compare final calculated activity and real activity. Measured error was defined as the following formula:

$$Error\ \% = \frac{|calcualted\ activity - real\ activity|}{real\ activity} \times 100 \quad (6)$$

RESULTS

Evaluation of the steps in SPECT quantification

Phantom contour was clearly outlined in reconstructed slices which was effective for image registration. In addition, two series of SPECT and planar images from Jaszczak phantom, with and without external ^{99m}Tc sources, revealed that less than 7% of total counts in ^{32}P Bremsstrahlung window were due to two external ^{99m}Tc sources.

Image registration process was user-based and has done with pair selection. Two evaluation coefficients, TO and DC, were 0.91±0.03 and 0.89±0.05, respectively.

Experimentally calculated effective linear attenuation coefficient was 0.13 cm^{-1} for ^{32}P. The bilinear HU to LAC curve for creating attenuation map is illustrated in figure 2. Non-uniform (right image) and uniform (left image) attenuation map of phantom is demonstrated in figure 3.

Figure 4 illustrates images of defined digital phantom with non-uniform attenuation map and five hot spots and background activity (activity

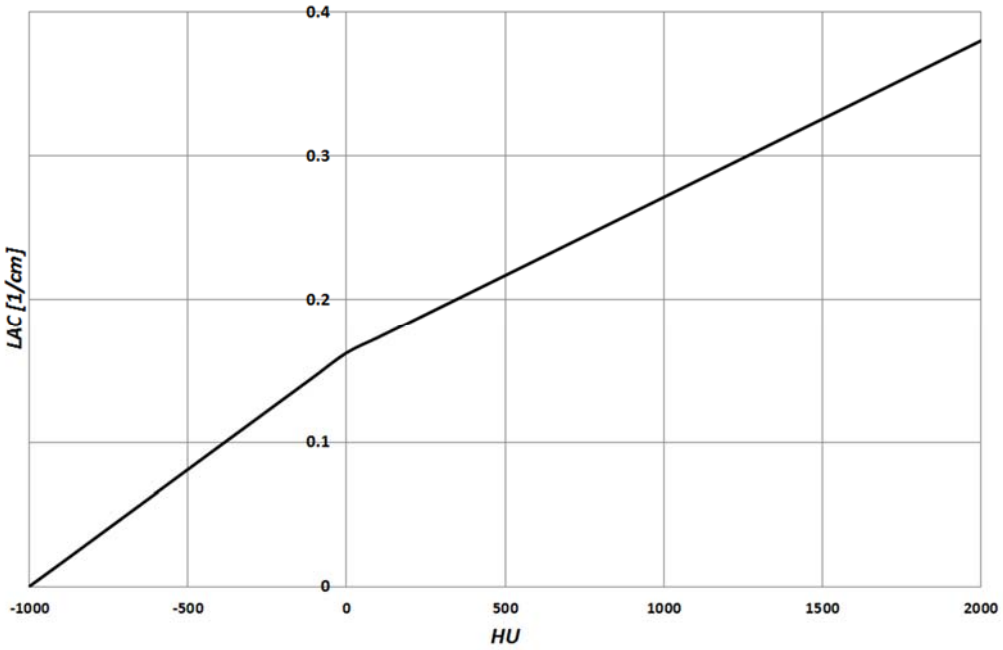

Figure 2. Hounsfield Unit (HU) to Linear Attenuation Coefficient (LAC) curve.

ratio of 5:1). Vertical profile at the middle of obtained images clearly shows quantitative difference between images before and after performing AC (figure 5). In this figure, the curve labeled "AC (EM)" represents the profile of reconstructed image with intrinsic attenuation correction during EM reconstruction, "Att. Free image" represents the true activity distribution (reference image), and "W/O AC" represents the profile of reconstructed image with MLEM technique but without any attenuation correction. One should consider that this graph has only the purpose of evaluating proposed intrinsic AC technique; hence we did not include Chang's AC technique here.

Results of SPECT and planar quantification

Experimentally measured system calibration factor using a petri dish containing known activity of ^{32}P was 0.324 counts/s/MBq. The calculated activity of SPECT phantom images was 35.33±2.9 MBq using Chang`s method and 47.79±1.66 MBq using EM method (table 1). Therefore, the Mean error for SPECT quantification was 28.14±5.89% and 2.8±2.58% using Chang`s and EM method, respectively. As a result, mean measured activity was statistically different between two SPECT methods as well as planar quantitation (P=0.0001).

Mean calculated activity using planar images and CVM was 64.28±2.66 MBq with mean error of 30.73±5.4%.

With respect to phantom identities of 9564.4 ml volume and 10.14 Kg mass, the mean calculated delivered dose to the entire phantom was 0.93±0.03 Gy using iterative method.

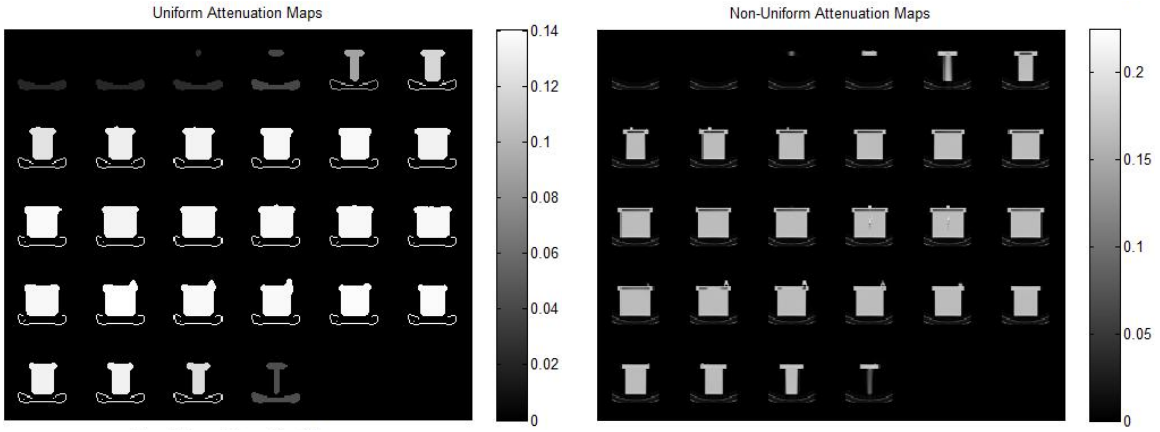

Figure 3. An example of non-uniform (right image) and uniform (left image) attenuation maps.

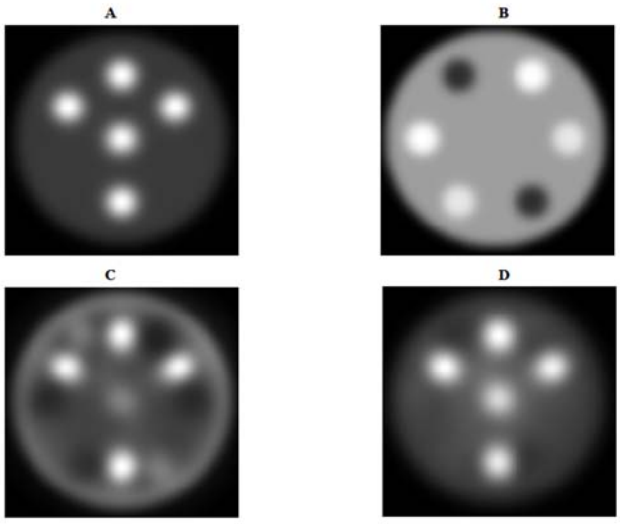

Figure 4. Images of defined digital phantom by SIMIND MC code. A. Image without attenuation effect, B. Attenuation map, C. Image with attenuation effect and D. Reconstructed image with compensation for attenuation effect.

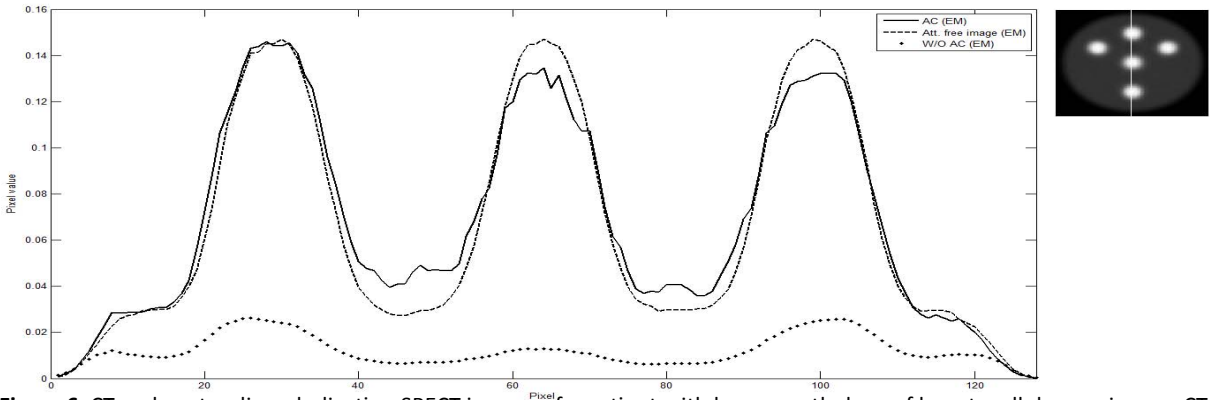

Figure 6. CT and post radioembolization SPECT images of a patient with known pathology of hepatocellular carcinoma. CT image shows two lesions in the right hepatic lobe. Reconstructed SPECT slices demonstrate successful distribution of radiotracer in both lesions after hepatic radioembolization with 259 MBq colloidal ^{32}P.

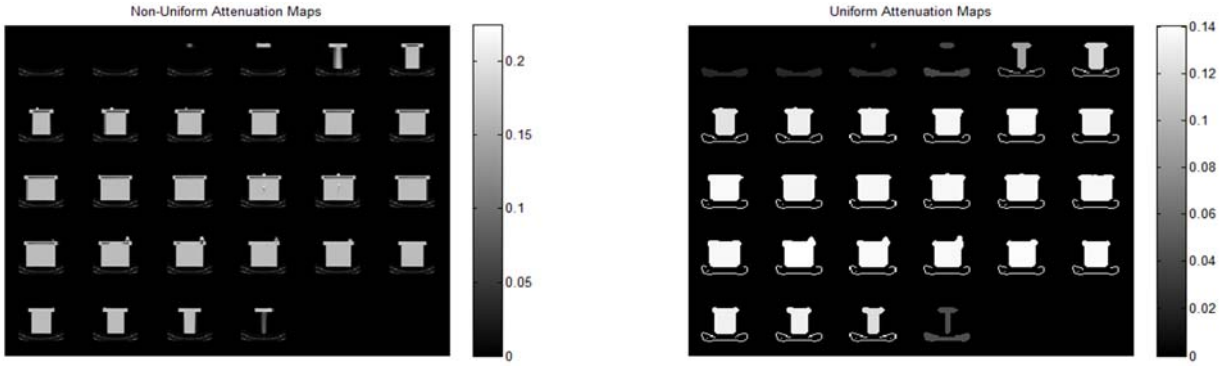

Figure 5. Profile curves of phantom image before and after performing AC by EM method.

Table 1. Calculated activity (MBq) from planar phantom images by CVM as well as SPECT phantom images using Chang`s and EM methods with the measured activity error in compared to real source activity of 49.17 MBq.

	Calculated activity [MBq] Chang`s method	Error (%)	Calculated activity [MBq] EM method	Error (%)	Calculated activity [MBq] planar
1	41.07	16.48	48.14	2.11	67.12
2	35.33	28.14	48.91	0.53	61.84
3	33.89	31.08	46.92	4.59	62.29
4	37.85	23.02	51.06	3.84	62.64
5	32.15	34.61	45.51	7.45	63.97
6	38.07	22.57	49.95	1.58	63.78
7	33.59	31.68	45.51	7.45	59.99
8	37.67	23.40	49.58	0.83	64.34
9	33.08	32.73	45.36	7.75	66.07
10	32.15	34.61	45.25	7.98	64.30
11	36.67	25.43	47.14	4.14	62.14
12	32.41	34.09	48.88	0.60	59.89
13	37.66	23.40	49.54	0.75	67.28
14	35.9	27.01	48.40	1.58	65.07
15	31.78	35.36	47.77	2.86	66.69
16	33.04	32.81	48.40	1.58	63.49
17	37.89	22.95	47.18	4.06	67.1
18	32.30	34.31	46.18	6.09	60.97
19	33.85	31.15	48.36	1.66	67.7
20	40.33	17.98	47.88	2.63	68.89

DISCUSSION

Image registration

In this study we used user-based image processing, however, quantitative Bremsstrahlung SPECT imaging has been evaluated for ^{90}Y-Microspheres [6-10] with more advanced SPECT/CT machines in the recent studies [25]. SPECT/CT not only demonstrates radiotracer distribution, but also improves registration part and attenuation correction algorithm for quantitative purposes [25]. While SPECT/CT facility is limited in few centers in Iran and some other countries, a simple practical method was examined in this study to register separate acquired SPECT and CT images and apply attenuation correction algorithm for subsequent delivered dose calculation after liver radioembolization.

In this study, the most practical algorithm [14, 26] was selected for Bremsstrahlung SPECT and CT image registration using external ^{99m}Tc sources to generate backscattered photons. Clear phantom contour and landmarks along Z axis improved the registration parts. TO and DC were 0.91±0.03 and 0.89±0.05, respectively, both completely acceptable and valid for image registration. In addition, compensation for backscatter photons, contributing to almost 7% of image activity, was performed. This technique can be implemented in patient studies, as well. Figure 6 shows an example of CT and post-radioembolization SPECT slices of a patient with hepatocellular carcinoma.

Activity determination

A study [7] performed on RSD torso phantom and a Jaszczak phantom filled with water for ^{90}Y with ESSE scatter correction method [27] for Bremsstrahlung photons and compensation for collimator-detector response showed that attenuation and scatter correction could reduce the difference of true and measured activity by approximately 11%, while there is more than 60% difference between true and measured activity in case of no correction. In addition, it indicated that compensation for collimator-detector response is not considerably effective on quantitative results. The estimated activity of Jaszczak phantom was within 4.4% of true activity in the present study, though no compensation for scatter photons or collimator-detector response was applied. Nevertheless, the accuracy of quantitation could be affected by increasing number of scattered photons in larger sources (e.g. liver), so further investigation is required.

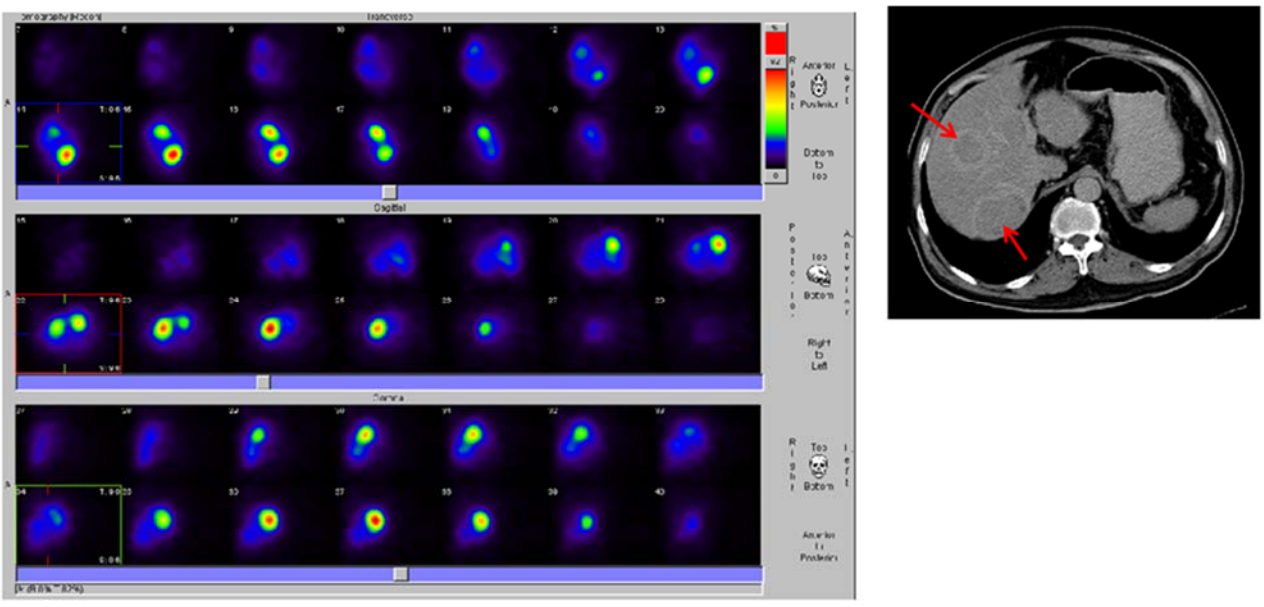

Figure 6.CT and post radioembolization SPECT images of a patient with known pathology of hepatocellular carcinoma. CT image shows two lesions in the right hepatic lobe. Reconstructed SPECT slices demonstrate successful distribution of radiotracer in both lesions after hepatic radioembolization with 259 MBq colloidal ^{32}P.

Many reports confirmed that accurate quantitative Bremsstrahlung SPECT imaging is possible even without performing compensation for scattered photons, at least in uniformly attenuating parts of the body such as abdomen and pelvis [10, 28]. It has been reported that accurate SPECT quantification could be obtained with compensation for attenuation effect using Chang`s method if body contour was well defined [10]. On the other hand, iterative reconstruction method with intrinsic AC algorithm was more successful to evaluate Bremsstrahlung SPECT images [7]. In the present study, mean measured activity error was 4% when intrinsic attenuation correction method (EM method) was applied to reconstructed transverse ^{32}P Bremsstrahlung slices of phantom images and was statistically more accurate than the first order post-processing Chang`s method which underestimates activity by average of 27.8%. It should be considered that activity calculation might have less accuracy within the patient's liver and tumors due to more complicated geometry than Jaszczak phantom and necessitates more assessment.

Measured activity error has been reported up to 13% in quantitative planar ^{90}Y Bremsstrahlung imaging of Alderson abdominal phantom [8] using effective point source method [29, 30] and CVM [15]. The other study reported that Bremsstrahlung planar quantification was feasible if proper compensation for background and overlap were implemented [6]. The present study was performed without any specific c ompensation for scatter photons, background counts, and overlap volumes in planar images, and it indicated that activity estimation using CVM without any physical correction might have quantification error of up to 29%. Also experimentally measured linear attenuation coefficient was 0.13 cm^{-1}.

CONCLUSION

This study revealed that quantitative ^{32}P Bremsstrahlung SPECT imaging with the applied algorithm is clinically practical and accurate for determining body contour when appropriate registration with CT and precise AC was performed even without sophisticated scatter correction.^{32}P Bremsstrahlung planar quantification may, however, needs further sophisticated compensations for more accurate results.

Consequently, Bremsstrahlung SPECT quantification could be simply applicable in clinical practice for the purpose of tumor dosimetry after liver radioembolization with pure beta emitters, specially when SPECT/CT machines are not convenient.

REFERENCES

1. Hamami ME, Poeppel TD, Muller S, Heusner T, Bockisch A, Hilgard P, *et al.* (2009) SPECT/CT with 99mTc-MAA in radioembolization with 90Y microspheres in patients with hepatocellular cancer. *J Nucl Med,* ***50(5):*** *688-92.*
2. Akhlaghpoor S, Aziz-Ahari A, Amoui M, Tolooee S, Poorbeigi H, Sheybani S (2012) Short-term effectiveness of radiochemoembolization for selected hepatic metastases with a combination protocol. *World J Gastroenterol,* ***18 (37):****5249-59.*
3. D'Asseler Y (2009) Advances in SPECT imaging with respect to radionuclide therapy. *Q J Nucl Med Mol Imaging,* ***53(3):*** *343-7.*
4. Kennedy A, Nag S, Salem R, Murthy R, McEwan AJ, Nutting C, *et al.* (2007) Recommendations for radioembolization of hepatic malignancies using yttrium-90 microsphere brachytherapy: a consensus panel report from the radioembolization brachytherapy oncology consortium. *Int J Radiat Oncol Biol Phys,* ***68(1):****13-23.*
5. Murthy R, Habbu A, Salem R (2006) Trans-arterial hepatic radioembolisation of yttrium-90 microspheres. *Biomed Imaging Interv J,* ***2(3):*** *e43.*
6. Minarik D, Ljungberg M, Segars P, Gleisner KS (2009) Evaluation of quantitative planar 90Y bremsstrahlung whole-body imaging. *Phys Med Biol,* ***54(19):*** *5873-83.*
7. Minarik D, Sjogreen Gleisner K, Ljungberg M (2008) Evaluation of quantitative (90)Y SPECT based on experimental phantom studies. *Phys Med Biol,* ***53(20):*** *5689-703.*
8. Shen S, DeNardo GL, Yuan A, DeNardo DA, DeNardo SJ (1994) Planar gamma camera imaging and quantitation of yttrium-90 bremsstrahlung. *J Nucl Med,* ***35(8):*** *1381-9.*
9. Siegel JA (1994) Quantitative bremsstrahlung SPECT imaging: attenuation-corrected activity determination. *J Nucl Med,* ***35(7):****1213-6.*
10. Siegel JA, Zeiger LS, Order SE, Wallner PE (1995) Quantitative bremsstrahlung single photon emission computed tomographic imaging: use for volume, activity, and absorbed dose calculations. *Int J Radiat Oncol Biol*

Phys, ***31(4):*** *953-8.*
11. Siegel JA, Thomas SR, Stubbs JB, Stabin MG, Hays MT, Koral KF, *et al.* (1999) MIRD pamphlet no. 16: Techniques for quantitative radiopharmaceutical biodistribution data acquisition and analysis for use in human radiation dose estimates. *J Nucl Med,* ***40(2):*** *37S-61S.*
12. Bruyant PP. (2002) Analytic and iterative reconstruction algorithms in SPECT. *J Nucl Med,* ***43(10):*** *1343-58.*
13. Chang LT (1978) A Method Attenuation Correction in Radionuclide Computed Tomography. *IEEE Trans Nucl Sci, NS-****25:*** *638-42.*
14. Siegel JA and Khan SH (1996) Body contour determination and validation for bremsstrahlung SPECT imaging. *J Nucl Med,* ***37(3):****495-7.*
15. Fleming JS (1979) A technique for the absolute measurement of activity using a gamma camera and computer. *Phys Med Biol,* ***24(1):*** *176-80.*
16. Siegel JA, Whyteellis S, Zeiger LS, Order SE, Wallner PE (1994) Bremsstrahlung SPECT imaging and volume quantitation with 32 phosphorus. *Antibody Immunoconjugates and Radiopharmaceuticals,****7(1):*** *1-10.*
17. Fleming JS (1989) A technique for using CT images in attenuation correction and quantification in SPECT. *Nucl Med Commun,* ***10(2):*** *83-97.*
18. Crum WR, Camara O, Hill DL (2006) Generalized overlap measures for evaluation and validation in medical image analysis. *IEEE Trans Med Imaging,* ***25(11):*** *1451-61.*
19. Dice LR (1945) *Measures of the Amount of Ecologic Association Between Species Ecology,* ***26:****297-302.*
20. Zijdenbos AP, Dawant BM, Margolin RA, Palmer AC (1994) Morphometric analysis of white-matter lesions in MR-images - method and validation. *IEEE Trans Med Imaging,* ***13(4):*** *716-24.*
21. Ljungberg M and Strand SE (1989) A Monte Carlo program for the simulation of scintillation camera characteristics. *Comput Methods Programs Biomed,* ***29(4):****257-72.*
22. Bai CY, Shao L, Da Silva AJ, Zhao Z (2003) A generalized model for the conversion from CT numbers to linear attenuation coefficients. *Ieee Transactions on Nuclear Science,* ***50(5):*** *1510-5.*
23. Berger MJ, Hubbell JH, Seltzer SM, Chang J, Coursey JS, Sukumar R, *et al.* XCOM: Photon Cross Sections Database. The National Institute of Standards and Technology (NIST) March 1998 [updated November 2010].
24. Canny J (1986) A computational approach to edge detection. *IEEE Trans Pattern Anal Mach Intell,* ***8(6):*** *679-98.*
25. Mansberg R, Sorensen N, Mansberg V, Van der Wall H (2007) Yttrium 90 Bremsstrahlung SPECT/CT scan demonstrating areas of tracer/tumour uptake. *Eur J Nucl Med Mol Imaging,* ***34(11):****1887.*
26. Parsai EI, Ayyangar KM, Dobelbower RR, Siegel JA (1997) Clinical fusion of three-dimensional images using Bremsstrahlung SPECT and CT. *J Nucl Med,* ***38(2):*** *319-24.*
27. Frey EC and Tsui BMW(Conference Record 1997)A new method for modeling the spatially-variant, object-dependent scatter response function in SPECT. In: DelGuerra A, editor. 1996 Ieee Nuclear Science Symposium - Conference Record, Vols 1-3. *Ieee Nuclear Science Symposium, p. 1082-6.*
28. Zanzonico PB, Bigler RE, Sgouros G, Strauss A (1989) Quantitative SPECT in radiation dosimetry. *Semin Nucl Med,* ***19(1):****47-61.*
29. DeNardo GL, DeNardo SJ, Macey DJ, Mills SL(1988) Quantitative Pharmacokinetics of Radiolabeled Monoclonal Antibodies for Imaging and Therapy in Patients. In: Srivastava SC, editor. Radiolabeled Monoclonal Antibodies for Imaging and Therapy. 152. New York: Plenum Press; 1988.
30. Macey DJ, DeNardo GL, DeNardo SJ (1990) A treatment planning program for radioimmunotherapy. *Front Radiat Ther Oncol,* ***24:****123-31; discussion 61-5.*